

Title	Gas- and particle-phase products from the photooxidation of acenaphthene and acenaphthylene by OH radicals
Authors	Riva, Matthieu;Healy, Robert M.;Flaud, Pierre-Marie;Perraudin, Emilie;Wenger, John C.;Villenave, Eric
Publication date	2017-11-30
Original Citation	Riva, M., Healy, R. M., Flaud, P.-M., Perraudin, E., Wenger, J. C. and Villenave, E. (2017) 'Gas- and particle-phase products from the photooxidation of acenaphthene and acenaphthylene by OH radicals', Atmospheric Environment, 151, pp. 34-44. doi:10.1016/j.atmosenv.2016.11.063
Type of publication	Article (peer-reviewed)
Link to publisher's version	10.1016/j.atmosenv.2016.11.063
Rights	© 2016 Elsevier Ltd. This manuscript version is made available under the CC-BY-NC-ND 4.0 license - <a href="http://creativecommons.org/licenses/by-nc-nd/4.0/">http://creativecommons.org/licenses/by-nc-nd/4.0/</a>
Download date	2023-05-05 01:49:28
Item downloaded from	<a href="http://hdl.handle.net/10468/3554">http://hdl.handle.net/10468/3554</a>



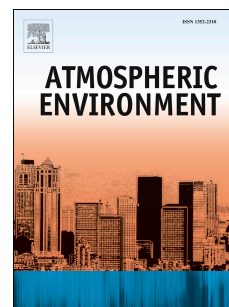
**UCC**

**University College Cork, Ireland**  
Coláiste na hOllscoile Corcaigh

# Accepted Manuscript

Gas- and particle-phase products from the photooxidation of acenaphthene and acenaphthylene by OH radicals

Matthieu Riva, Robert M. Healy, Pierre-Marie Flaud, Emilie Perraudin, John C. Wenger, Eric Villenave



PII: S1352-2310(16)30953-0

DOI: [10.1016/j.atmosenv.2016.11.063](https://doi.org/10.1016/j.atmosenv.2016.11.063)

Reference: AEA 15056

To appear in: *Atmospheric Environment*

Received Date: 23 September 2016

Revised Date: 17 November 2016

Accepted Date: 28 November 2016

Please cite this article as: Riva, M., Healy, R.M., Flaud, P.-M., Perraudin, E., Wenger, J.C., Villenave, E., Gas- and particle-phase products from the photooxidation of acenaphthene and acenaphthylene by OH radicals, *Atmospheric Environment* (2016), doi: 10.1016/j.atmosenv.2016.11.063.

This is a PDF file of an unedited manuscript that has been accepted for publication. As a service to our customers we are providing this early version of the manuscript. The manuscript will undergo copyediting, typesetting, and review of the resulting proof before it is published in its final form. Please note that during the production process errors may be discovered which could affect the content, and all legal disclaimers that apply to the journal pertain.

# Gas- and particle-phase products from the photooxidation of acenaphthene and acenaphthylene by OH radicals

*Matthieu Riva,<sup>†,‡,#</sup> Robert M. Healy,<sup>§,¥</sup> Pierre-Marie Flaud,<sup>†,‡</sup> Emilie Perraudin,<sup>†,‡</sup> John C.  
Wenger,<sup>\*,§</sup> Eric Villenave<sup>\*,†,‡</sup>*

<sup>†</sup> Univ. Bordeaux, EPOC, UMR 5805, F-33405 Talence cedex, France

<sup>‡</sup> CNRS, EPOC, UMR 5805, F-33405 Talence cedex, France

<sup>§</sup> Department of Chemistry and Environmental Research Institute, University College Cork,  
Cork, Ireland

<sup>#</sup> Now at the Department of Physics, PO Box 64, 00014 University of Helsinki, Finland

<sup>¥</sup> Now at Environmental Monitoring and Reporting Branch, Ontario Ministry of the  
Environment and Climate Change, Toronto, Canada

\* Corresponding Authors:

Email - e.villenave@epoc.u-bordeaux1.fr; Phone – 33-5-4000-6350

Email - j.wenger@ucc.ie; Phone – 353-2-1490-2454

## Abstract

This work is focused on the gas-phase oxidation of acenaphthylene and acenaphthene by OH radicals and associated secondary organic aerosol (SOA) formation under low and high-NO<sub>x</sub> conditions. Experiments were carried out in an atmospheric simulation chamber using a proton transfer reaction time-of-flight-mass spectrometer (PTR-TOF-MS) and an aerosol time-of-flight-mass spectrometer (ATOFMS) to chemically characterize the gas- and particle-phase products, respectively. Due to the structures of these two aromatic compounds, the proposed chemical mechanisms exhibit some differences. In the case of acenaphthene, H-atom abstraction from the saturated cyclopenta-fused ring was found to be competitive with the OH-addition to the aromatic rings. During the photooxidation of acenaphthene using nitrous acid (HONO), aromatic ring-opening products such as indanone and indanone carbaldehyde, generated through OH addition to the aromatic ring, were formed in higher yields compared to low-NO<sub>x</sub> conditions. In the case of acenaphthylene, OH addition to the unsaturated cyclopenta-fused ring was strongly favored. Hence, ring-retaining species such as acenaphthenone and acenaphthenequinone, were identified as the main reaction products in both gas- and particle-phases, especially under high-NO<sub>x</sub> conditions. Subsequent SOA formation was observed in all experiments and SOA yields were determined under low/high-NO<sub>x</sub> conditions to be 0.61/0.46 and 0.68/0.55 from the OH-initiated oxidation of acenaphthylene and acenaphthene, respectively.

## 1. Introduction

Atmospheric fine particulate matter (PM<sub>2.5</sub>, aerosol with aerodynamic diameters less than 2.5  $\mu\text{m}$ ) plays a key role in air quality and climate change, and is associated with damaging effects on human health (Pope III and Docherty, 2006; Hallquist et al., 2009). Globally, the largest mass fraction of PM<sub>2.5</sub> is organic (up to 90% in some locations) and is dominated by secondary organic aerosol (SOA). Formation of SOA mainly results from the formation of gas-phase products with low vapor pressures from the oxidation of volatile organic compounds (VOCs) (Hallquist et al., 2009). The anthropogenic contribution to global SOA formation is estimated to be small, actually around 10% (Kroll et al., 2008). SOA formation from anthropogenic sources is, however, suggested to be higher than currently predicted (Volkamer et al., 2006; Hallquist et al., 2009). In order to explain the current discrepancy between the mass of aerosols measured in different atmospheres and the mass predicted by atmospheric models, some studies have suggested that other sources of SOA are not yet identified or well characterized (Kroll et al., 2008; Hallquist et al., 2009). Among them, heterogeneous chemistry (formation of oligomers and organosulfates) (Surratt et al., 2008; Pye and Pouliot, 2012) and the contribution of intermediate volatility organic compounds (IVOCs) to SOA formation have been proposed (Robinson et al., 2007; Tkacik et al., 2012). It is worth noting that recent studies have also underlined that reactive uptake and/or multiphase chemistry of water-soluble volatile organic compounds, such as glyoxal, in wet acidic aerosols or cloud droplets could be an important source of SOA (Galloway et al., 2009; Ervens et al., 2011; Pye et al., 2013; Marais et al., 2016). Nevertheless, a large part of the underestimation in urban areas, due to the non-considered IVOC contribution to SOA formation, comes from the involvement of alkanes and polycyclic aromatic hydrocarbons (PAHs) (Tkacik et al., 2012). Much of the current efforts in the research community are focused on trying to identify these missing or misrepresented SOA sources.

PAHs are emitted into the atmosphere from incomplete combustion processes of organic materials and have been identified as major components in traffic and wood burning emissions. The PAHs with less than four aromatic rings exist mainly in the gaseous phase and can undergo photooxidation processes with different atmospheric oxidants (Atkinson and Aschmann, 1988; Sasaki et al., 1998; Keyte et al., 2013; Zhou and Wenger, 2013a,b; Riva et al., 2014). When oxidized, these compounds have been shown to produce large range of oxygenated and nitro compounds with high molecular weights (Sasaki et al., 1998; Reisen and

Arey, 2002; Lee and Lane, 2009; Kautzman et al., 2010; Kleindienst et al., 2012; Zhou et al., 2013a,b; Riva et al., 2015a,b,c, 2016). Although PAHs are potentially carcinogenic and mutagenic (Atkinson and Arey, 1994) some of their oxidation products present a larger toxicity than their parent hydrocarbons (Lin et al., 2005). Gas-phase products can partition to the particle phase and participate in SOA formation (Chan et al., 2009; Kautzman et al., 2010; Shakya et al., 2010; Kleindienst et al., 2012; Riva et al., 2015a; Chen et al., 2016; Riva et al., 2016). A few studies have previously reported the importance of naphthalene gas phase photooxidation in SOA formation (Chan et al., 2009; Kleindienst et al., 2012). Other gaseous PAHs have, however received less attention. Acenaphthylene and acenaphthene are fairly unique among PAHs in that they contain a carbon-carbon double bond and a saturated carbon-carbon bond, respectively, in their structure that enables them to react quickly with all atmospheric oxidants including OH and NO<sub>3</sub> radicals, Cl atoms and O<sub>3</sub> (Atkinson and Aschmann, 1988; Reisen and Arey, 2002; Zhou and Wenger, 2013a,b; Riva et al., 2014). Acenaphthylene and acenaphthene were identified in both indoor and outdoor atmospheres and in large concentrations in certain areas (Chang et al., 2006; Ho et al., 2009). The concentration of both PAHs (greater than 20-30 ng m<sup>-3</sup>) could be even comparable to that of naphthalene in certain urban atmospheres (Dejean et al., 2009; Hanedar et al., 2014) suggesting that acenaphthylene and acenaphthene might contribute to SOA formation in such areas. Large rate constants for the reaction of acenaphthene ( $(7.69 \pm 1.91) \times 10^{-11}$ ) and acenaphthylene ( $(1.14 \pm 0.08) \times 10^{-10}$ ) in cm<sup>3</sup> molecule<sup>-1</sup> s<sup>-1</sup>) with OH radicals have been previously reported (Atkinson and Aschmann, 1988; Zhou and Wenger, 2013a,b). These previous efforts underline the potential importance of the OH initiated oxidation of acenaphthylene and acenaphthene in the atmospheric chemistry of PAHs. Indeed, it has been shown that the reactivity of aromatic hydrocarbons is dominated by their reactions with the OH radicals in the atmosphere (Calvert et al., 2002; Estève et al., 2003; Atkinson and Arey, 2007). Although the OH-initiated oxidation of PAHs has been studied previously, the impact of NO<sub>x</sub> concentration on the reactivity of PAHs remains poorly documented. Only two studies on the oxidation of naphthalene performed under high- and low-NO<sub>x</sub> conditions, have been reported hitherto (Kautzman et al., 2009; Kleindienst et al., 2012). Previous works have determined the rate constants and oxidation products for the photooxidation of acenaphthene and acenaphthylene in the presence of NO<sub>x</sub> (Atkinson and Aschmann, 1988; Reisen and Arey, 2002; Zhou and Wenger, 2013a,b). In addition, Shakya and Griffin (2010) have, for the first time, reported the SOA yields arising from these reactions. These results highlight the propensity for both PAHs to participate in SOA formation and only partial mechanisms were

proposed in these previous studies. However, some discrepancies remain and further work is needed to clarify the reaction products as well as the chemical mechanisms leading to SOA formation.

In this work, we performed a series of simulation chamber experiments to identify products arising from the photooxidation of acenaphthylene and acenaphthene under low- and high- $\text{NO}_x$  conditions using state-of-the-art mass spectrometry techniques for on-line analysis of both gaseous (proton transfer reaction time-of-flight-mass spectrometer) and particulate (aerosol time-of-flight-mass spectrometer) phases. Based on these approaches, extended and improved reaction mechanisms for the OH-initiated oxidation of acenaphthylene and acenaphthene are now proposed. SOA growth and yields are determined in both cases to evaluate the importance of the photooxidation of acenaphthene and acenaphthylene in SOA formation.

## 2. Experimental section

Experiments were performed at room temperature ( $293 \pm 2$  K) and atmospheric pressure in the 3910 L atmospheric simulation chamber at University College Cork, which is described in detail elsewhere (Thüner et al., 2004). Briefly, it is a cylinder consisting of a Teflon FEP foil tube closed with aluminum plates covered with Teflon FEP foil. The chamber is equipped with fans to ensure rapid mixing of reactants and is surrounded by 16 lamps (Philips TL12, 40W) with an emission maximum at 310 nm and 12 lamps (Philips TL05, 40 W) with an emission maximum at 360 nm (Kourtchev et al., 2009). Before each experiment, the chamber is cleaned by flushing with dried purified air and photolysis of added ozone (ca. 1 ppmv) until the particle number concentration is below  $200 \text{ cm}^{-3}$ . The flushing also reduces the levels of  $\text{NO}_x$  and non-methane hydrocarbons to  $< 10$  ppbv. The mixing ratios of  $\text{NO}_x$  and  $\text{O}_3$  are measured using standard automated gas analyzers (Thermo Model 42i and 49i respectively). The temperature and water concentration in the chamber were monitored by a dew point meter (Vaisala DM70). The relative humidity in the chamber was typically less than 1% for the experiments with HONO and less than 5% for experiments carried out with  $\text{H}_2\text{O}_2$ .

Acenaphthylene (Sigma-Aldrich, 99%) and acenaphthene (Sigma-Aldrich, 99%) were introduced into the chamber by flowing dry purified air throughout a heated Pyrex glass bulb containing a known amount of the solid compound sufficient to produce PAH mixing ratios around 300 ppb (Table S1). The PAHs and gas-phase oxidation products were monitored

during the experiments using a proton transfer reaction - time of flight - mass spectrometer (PTR-TOF-MS, Kore Technology Ltd.). Details of the instrument and its operating principle are given in Cappelin et al. (2012). Briefly,  $\text{H}_3\text{O}^+$  is produced in a hollow cathode ion source and reacts with organic compounds (M) that have a higher proton affinity than  $\text{H}_2\text{O}$  to generate positively charged ions  $(\text{M} + \text{H})^+$ , which are subsequently detected using a time-of-flight mass spectrometer. The PTR-TOF-MS was operated over the  $m/z$  range 0-300 using a sampling time of 1 min. The decay of the PAHs was monitored by following the protonated molecular ions:  $m/z$  153 (acenaphthylene) and  $m/z$  155 (acenaphthene). Quantification of identified products was not possible due to difficulty obtaining accurate concentrations in the gas phase during the PTR-TOF-MS calibration.

Experiments were carried out in order to study the oxidation of acenaphthylene and acenaphthene under high- and low- $\text{NO}_x$  conditions. Nitrous acid (HONO) was used as an OH radical precursor and was generated by adding 0.5 mL of 1 wt % aqueous sodium nitrite ( $\text{NaNO}_2$ , Sigma-Aldrich, 97%) dropwise into 30 mL of 30 wt % sulfuric acid (Sigma-Aldrich, 99.9%) in a glass bulb (Cox, 1974). Purified air was flowed through the bulb, delivering HONO to the chamber. The injection of HONO was stopped when the concentration of nitrogen dioxide reached about 200 ppb in the chamber. Hydrogen peroxide ( $\text{H}_2\text{O}_2$ , Sigma-Aldrich, 50 wt %) was used to generate OH radicals without  $\text{NO}_x$ . 60  $\mu\text{L}$  was injected into the glass bulb followed by slight heating. Purified air was passed through the bulb to introduce  $\text{H}_2\text{O}_2$  into the chamber.

The formation and growth of SOA was monitored using a scanning mobility particle sizer (SMPS, TSI model 3034): size distribution, number and mass concentrations were determined for all experiments, assuming an SOA density of  $1.4 \text{ g cm}^{-3}$  (Chan et al., 2009; Shakya et al., 2010). SOA chemical composition was investigated using an aerosol time-of-flight mass spectrometer (ATOFMS, TSI model 3800), which has been described in detail elsewhere (Gard et al., 1997). Briefly, single particles are sampled through a critical orifice and focused into a tight beam in the aerodynamic lens before transmission to the sizing region. The velocity of the particles is measured using two continuous wave diode-pumped Nd:YAG lasers operating at 532 nm. The time between these two scattering events is used to obtain the aerodynamic size. Aerosols are then transmitted to the ionization region of the instrument where desorption/ionization is performed by a Nd:YAG laser at 266 nm. This ablation process generates high densities of charges, in which intermolecular interactions and matrix effects



often determine the ion distribution, making quantitative calibration of mass spectra extremely difficult (Zelenyuk and Imre, 2005). Due to instrumental issues only positive ions were detected using the ATOFMS. It is important to note, however, that PAHs are mainly detected as positive ions (Silva and Prather, 2000; Zimmermann et al., 2003). The laser is typically operated with an output energy of around 1 mJ per pulse. However, as described elsewhere lower pulse energies were used in this work to reduce fragmentation of the organic constituents in the aerosol (Zimmermann et al., 2003; Gross et al., 2000; 2005).

Based on the measured decay of PAH and known rate constants for reaction with OH (unit:  $\text{cm}^3 \text{ molecule}^{-1} \text{ s}^{-1}$ ):  $(7.69 \pm 1.91) \times 10^{-11}$  and  $(1.14 \pm 0.08) \times 10^{-10}$  for acenaphthene and acenaphthylene, respectively (Atkinson and Aschmann, 1988; Brubaker and Hites, 1998; Banceau et al., 2001; Reisen and Arey, 2002; Zhou and Wenger, 2013a,b) the initial OH radical concentrations using  $\text{H}_2\text{O}_2$  and HONO as precursor were (unit:  $\text{molecule cm}^{-3}$ ):  $(3.47 \pm 0.32) \times 10^6$  and  $(8.34 \pm 1.36) \times 10^6$  respectively.

### 3. Results and discussion

#### 3.1 Acenaphthylene photooxidation

The PTR-TOF-MS measurements performed in acenaphthylene photooxidation experiments carried out under low and high- $\text{NO}_x$  conditions revealed 6 product peaks with  $m/z$  values reported in Table S2. The temporal profiles of the identified ions are proposed in Figure 1. Most of the reaction products are similar to those previously reported or for reactions performed in the same chamber but using Cl atoms or  $\text{O}_3$  to initiate oxidation (Reisen and Arey, 2002; Zhou and Wenger, 2013b; Riva et al., 2015a; Riva et al., 2016). Based on existing knowledge of the gas-phase chemistry of acenaphthylene, the peak at  $m/z$  185 is assigned to the protonated molecular ion  $(\text{M} + \text{H})^+$  of naphthalene-1,8-dicarbaldehyde ( $\text{C}_{12}\text{H}_8\text{O}_2$ ) and a dialdehyde formed from OH addition to the aromatic rings. Previous studies have reported large yields of both compounds from the photooxidation of acenaphthylene in the presence of  $\text{NO}_x$ . The protonated ion at  $m/z$  185 may have, however, more than 2 isomers. Indeed, as discussed below and proposed in Scheme 1, formation of a protonated ion at  $m/z$  183 ( $\text{C}_{12}\text{H}_6\text{O}_2$ ) and tentatively assigned as acenaphthenequinone cannot be explained by solely the gas-phase oxidation of acenaphthenone ( $\text{C}_{12}\text{H}_8\text{O}$ ). Indeed, the abundance of protonated ion at  $m/z$  169 is likely too weak to explain the large signal observed for acenaphthenequinone in the particulate phase (Figure 1). Therefore, formation of  $\text{C}_{12}\text{H}_6\text{O}_2$

might also proceed through the gas-phase oxidation of hydroxy-acenaphthenone as tentatively proposed in Scheme 1. Signals for the protonated ions at  $m/z$  169 and 185 decrease significantly after ca. 4000 s reaction time (Figure 1), suggesting that both primary reaction products undergo further gas-phase oxidation and/or photolysis leading to secondary generation compounds (Scheme 1). For instance, naphthalene-1,8-dicarbaldehyde may react further with OH radicals or be photodissociated as observed for other aromatic aldehydes (Wang et al., 2006).

Although the different compounds identified for each set of experiments were identical under high- or low- $\text{NO}_x$  conditions, their abundances were very different. As presented in Figure 1, the abundances of ring-opening products (e.g. oxaacenaphthylene-2-one, 1,8-naphthalic anhydride and 1,8-naphthalaldehydic acid) differ depending on the OH radical precursor. Moreover, the high signals of small fragment ions detected by the ATOFMS (Figure 2) at  $m/z$  39 ( $\text{C}_3\text{H}_3^+$ ), 51 ( $\text{C}_4\text{H}_3^+$ ), 63 ( $\text{C}_5\text{H}_3^+$ ), 75 ( $\text{C}_6\text{H}_3^+$ ), 77 ( $\text{C}_6\text{H}_5^+$ ) and 115 ( $\text{C}_9\text{H}_7^+$ ) highlight the presence of ring-opening products in the particulate phase, as demonstrated in previous studies using an ATOFMS at low laser energy (Riva et al., 2015a; Gross et al., 2000; 2005). The higher yield of ring opening products such as oxaacenaphthylene-2-one, 1,8-naphthalic anhydride and 1,8-naphthalaldehydic acid in the gas phase (Figure 1) is consistent with the higher signals for small fragment ions in the ATOFMS spectra (Figure 2), suggesting that formation of ring-opening products is likely enhanced under low- $\text{NO}_x$  conditions. This observation is in contrast with experiments performed in the presence of  $\text{NO}_x$ . In that case, ring-retaining species are enhanced, as revealed by the relatively larger abundances of acenaphthenone (or its enol-form) and acenaphthenequinone (Figures 1 and 2) in both phases, during the oxidation of acenaphthylene in the presence of HONO. It is worth noting that no nitro compounds were identified in either gas or particle phases. Previous studies have, however, reported the formation of nitro-products during the photooxidation of acenaphthylene, but with very low yields, which likely explains the absence of nitro-products in the mass spectra collected in this work (Arey et al., 1989; Reisen and Arey, 2002; Zhou and Wenger, 2013b).

An extended reaction mechanism for the gas-phase oxidation of acenaphthylene is proposed in Scheme 1. It is based on the PTR-TOF-MS data obtained in this work and also builds on the results from previous experimental studies (Reisen and Arey, 2002; Zhou and Wenger, 2013b). Oxidation of acenaphthylene is energetically favored at the unsaturated

cyclopenta-fused ring as highlighted in previous experimental (Atkinson and Aschmann, 1988; Reisen and Arey, 2002; Zhou and Wenger, 2013b; Riva et al., 2015a; Riva et al., 2016) and theoretical studies (Dang et al., 2015). This double bond exhibits high reactivity and explains the higher reactivity of acenaphthylene with atmospheric oxidants relative to other PAHs. Hence acenaphthylene photooxidation is governed by the OH addition at the unsaturated cyclopenta-fused ring. Due to the absence in our experiments of any nitro compounds and the very small yields reported in previous work, the OH-adduct is expected to mainly react with O<sub>2</sub>. OH-acenaphthylene adduct could then lead to a peroxy radical (RO<sub>2</sub>) (C<sub>12</sub>H<sub>9</sub>O<sub>3</sub><sup>•</sup>) and to acenaphthenone (and/or its enol-form). It has been reported that for simple aldehydes and ketones, the keto form is the most stable and thus the equilibrium is likely directed to the acenaphthenone (March, 1985). C<sub>12</sub>H<sub>9</sub>O<sub>3</sub><sup>•</sup> could then react with NO or go through its self- /cross-reactions leading to the alkoxy radical (C<sub>12</sub>H<sub>9</sub>O<sub>2</sub><sup>•</sup>). Two different pathways are proposed for the fate of C<sub>12</sub>H<sub>9</sub>O<sub>2</sub><sup>•</sup>, which appear to be as expected NO<sub>x</sub> dependent. Firstly, the ring-retaining channel could produce hydroxy-acenaphthenone, which could further react and lead to acenaphthenequinone (Scheme 1). As discussed above, this pathway appears to be likely favored in the presence of NO<sub>x</sub> due to the relatively lower abundance of small fragment ions in the mass spectrum of the ATOFMS as well as the larger presence of ring-retaining products in both gas and particulate phases (Figures 1 and 2). Secondly, C<sub>12</sub>H<sub>9</sub>O<sub>2</sub><sup>•</sup> can proceed through the ring-opening pathway occurring by C<sub>1</sub>-C<sub>2</sub> bond cleavage. As shown in Scheme 1, this reaction pathway leads exclusively to ring-opening products, which appear to be favored under low-NO<sub>x</sub> conditions. Naphthalene-1,8-dicarbaldehyde and 1,8-naphthalaldehydic acid (C<sub>12</sub>H<sub>8</sub>O<sub>3</sub>) are the two main primary products arising from this ring-opening pathway and further react as shown in Figure 2 and proposed in Scheme 1. As discussed above and reported in previous works (Zhou and Wenger, 2013b; Riva et al., 2015a,b), naphthalene-1,8-dicarbaldehyde can yield 1,8-naphthalic anhydride from H-atom abstraction of the aldehydic function, which would result in the formation of an RO<sub>2</sub> radical (C<sub>12</sub>H<sub>7</sub>O<sub>4</sub><sup>•</sup>). Similarly to phthalaldehyde, naphthalene-1,8-dicarbaldehyde could undergo photodissociation, leading to 1,8-naphthalic anhydride (Wang et al., 2006; Riva et al., 2015b). C<sub>12</sub>H<sub>7</sub>O<sub>4</sub><sup>•</sup> could then react with NO or RO<sub>2</sub> and form an acyl-oxy radical (C<sub>12</sub>H<sub>7</sub>O<sub>3</sub><sup>•</sup>). The chemistry of the resulting C<sub>12</sub>H<sub>7</sub>O<sub>3</sub><sup>•</sup> radical could proceed through the bicyclic peroxy radical route in a fashion analogous to that proposed in Scheme 1. C<sub>12</sub>H<sub>7</sub>O<sub>3</sub><sup>•</sup> radical could also decarboxylate quickly (Chacon-Madrid et al., 2013) and the resulting radical would react with O<sub>2</sub> leading to the formation of another RO<sub>2</sub> radical (C<sub>11</sub>H<sub>7</sub>O<sub>3</sub><sup>•</sup>). As

presented in Scheme 1 and previously proposed,  $C_{11}H_7O_3^{\bullet}$  could undergo cyclization and lead to the formation of oxaacenaphthylene-2-one (Zhou and Wenger, 2013b).

It is important to point out that  $O_3$  formation ( $\sim 20$  ppb final concentration) was observed during the experiments carried out with HONO from the photolysis of  $NO_2$ . Due to the high reactivity of acenaphthylene with ozone ((acenaphthylene +  $O_3$ );  $k = 3.99 \times 10^{-16} \text{ cm}^3 \text{ molecule}^{-1} \text{ s}^{-1}$ ),  $O_3$  might have participated in the formation of oxygenated species and acenaphthylene depletion (Zhou and Wenger, 2013b). Due to the large UV- absorption band overlap of acenaphthylene with ozone at wavelengths between 240 and 260 nm (Zander, 1969) it was not possible to determine an accurate contribution of ozone in the oxidation of acenaphthylene. Riva et al. (2016) recently reported that a secondary ozonide ( $C_{12}H_8O_3$ ) is the main gas phase product arising from ozonolysis of acenaphthylene. In the high- $NO_x$  experiments, the product ion corresponding to  $C_{12}H_8O_3$  was observed in very low abundances (i.e.  $< 70$  counts) indicating that the contribution of ozonolysis can be considered to be negligible in the photo-oxidation experiments performed in this work.

### 3.2 Acenaphthene photooxidation.

Ten oxidation products from the reaction of OH radicals with acenaphthene were identified by PTR-TOF-MS and the temporal profiles for the most abundant peaks are presented in Figure 3. These product peaks at  $m/z$  133, 161, 169 and 177 were tentatively assigned to protonated molecular ions of indanone ( $C_9H_8O$ ), indanone carbaldehyde ( $C_{10}H_8O_2$ ), acenaphthenone ( $C_{12}H_8O$ ) and oxoindan-carboxylic acid ( $C_{10}H_8O_3$ ), respectively. Among these 4 products, indanone carbaldehyde and acenaphthenone have been previously observed from the OH-initiated oxidation of acenaphthene under high- $NO_x$  conditions (Reisen and Arey, 2002; Zhou and Wenger, 2013a). For instance, Reisen and Arey (2002) reported significant formation of indanone carbaldehyde and estimated yields at 14-37%. Four other protonated ions were observed at  $m/z$  171, 183, 185 and 199 but in weaker abundance and were tentatively assigned, based on existing knowledge of the gas-phase chemistry of acenaphthene, to acenaphthenol ( $C_{12}H_{10}O$ ), acenaphthequinone ( $C_{12}H_6O_2$ ), naphthalene-1,8-dicarbaldehyde ( $C_{12}H_8O_2$ ) and 1,8-naphthalic anhydride ( $C_{12}H_6O_3$ ), respectively. Finally, weak signals at  $m/z$  187 and 200 measured only in the experiments performed in the presence of  $NO_x$  were tentatively assigned to a dialdehyde ( $C_{12}H_{10}O_2$ ) and nitroacenaphthene ( $C_{12}H_9NO_2$ ). Proposed products, and the ions used for their identification, are reported in Table S3.

The different products determined in this work are similar to those identified in previous studies or during other experiments on acenaphthene performed in the same environmental chamber but using Cl atoms as radical precursors (Reisen and Arey, 2002; Zhou and Wenger, 2013a; Riva et al., 2015a). As observed in the case of the photooxidation of acenaphthylene, the abundances of the different products were highly dependent on the  $\text{NO}_x$  concentrations. The temporal profiles of the main compounds identified in the gas phase were very different as presented in Figure 3. For example, formation of indanone and indanone carbaldehyde during acenaphthene photooxidation under high- $\text{NO}_x$  conditions was higher, while their abundances remained low in the absence of  $\text{NO}_x$ . Moreover, the protonated signal for acenaphthenone, which appears to be the main oxidation product from the photooxidation of acenaphthene under low- $\text{NO}_x$  conditions, was significantly higher compared to the experiments carried out in the presence of  $\text{NO}_x$ . These observations highlight that oxidation pathways or branching ratios highly depend on the  $\text{NO}_x$  concentration. Contrary to the acenaphthylene system, ATOFMS spectra for acenaphthene SOA (Figure 4) reveal high abundances of small fragment ions under low- and high- $\text{NO}_x$  conditions, suggesting a high contribution of aromatic ring-opening products. Thus, abundances of fragment ions in ATOFMS spectra cannot be used to distinguish reaction pathways. Several species have been identified in both the gas and particulate phases, corroborating a significant formation of aromatic ring-opening products (Reisen and Arey, 2002; Zhou and Wenger, 2013a).

A proposed extended reaction mechanism for the gas-phase oxidation of acenaphthene is presented in Scheme 2. It is based on the PTR-TOF-MS data obtained in this work and also builds on the results from previous experimental studies (Reisen and Arey, 2002; Zhou and Wenger, 2013a). The reaction of OH radicals with acenaphthene can, in principle, proceed via three possible pathways: OH addition to the aromatic rings, H-atom abstraction from the aromatic ring and H-atom abstraction from the saturated cyclopenta-fused ring. However, H-atom abstraction from the aromatic rings has been demonstrated to be negligible compared to OH addition for the oxidation of aromatic compounds (Calvert et al., 2002). Formation of aromatic ring-opened dicarbonyls, such as indanone carbaldehyde or dialdehyde, is proposed as shown in Scheme 2 to occur through OH addition to the aromatic rings followed by the reaction of the OH-acenaphthene adduct with  $\text{O}_2$  and further ring cleavages (Reisen and Arey, 2002). In this work, indanone carbaldehyde was observed as the major compound arising from this OH-addition pathway. It is important to mention that secondary chemistry has not been discussed in previous work, however, as presented in Figure 3, primary products

undergo further oxidation and lead to secondary products, including indanone and oxoindan-carboxylic acid (Scheme 2).

The initial H-atom abstraction by OH radicals is followed by addition of O<sub>2</sub> leading to a RO<sub>2</sub> radical (C<sub>12</sub>H<sub>9</sub>O<sub>2</sub><sup>•</sup>). Subsequent reactions with NO or RO<sub>2</sub> radicals proceed via two pathways; (i) the molecular channel, which results in equimolar amounts of acenaphthenone and acenaphthenol, and (ii) the radical channel which produces an RO radical (C<sub>12</sub>H<sub>9</sub>O<sup>•</sup>). C<sub>12</sub>H<sub>9</sub>O<sup>•</sup> can then further react with O<sub>2</sub> and lead to acenaphthenone as the sole product. As proposed in Scheme 2 an alternative pathway, i.e. C-C bond cleavage of the C<sub>12</sub>H<sub>9</sub>O<sup>•</sup> radical followed by further oxidation could lead to the formation of naphthalene-1,8-dicarbaldehyde. As described previously in the case of acenaphthylene, naphthalene-1,8-dicarbaldehyde could further react or be photolyzed and lead to 1,8-naphthalic anhydride from the H-atom abstraction of the aldehydic function. It is important to note that previous studies did not consider this channel and attributed the formation of acenaphthequinone, naphthalene-1,8-dicarbaldehyde and 1,8-naphthalic anhydride to analytical artifacts or from reactions with acenaphthene impurities (Reisen and Arey, 2002; Sauret-Szczepanski and Lane, 2004). Recently, Zhou and Wenger (2013a) investigated these potential analytical artifacts and demonstrated the formation of naphthalene-1,8-dicarbaldehyde during acenaphthene photooxidation. Acenaphthenone, acenaphthequinone and 1,8-naphthalic anhydride were also previously identified, ruling out the formation of these compounds as analytical artifacts. Moreover, the abundances of these products observed in this work cannot be explained by reactions of OH radicals or ozone with small amounts of acenaphthene impurities (e.g. acenaphthylene, < 1%). Hence, our results complement those obtained by Zhou and Wenger (2013a) highlighting the competition between OH addition to the aromatic rings and H-atom abstraction from the cyclopenta-fused ring.

The competition between these two pathways appears to be different depending on the NO<sub>x</sub> concentration. As shown above, the relative abundances of the gas phase products were very different in the presence and absence of NO<sub>x</sub> (Figure 3). In the absence of NO<sub>x</sub>, the products from the OH-addition pathways (i.e. indanone, indanone carbaldehyde and oxoindan-carboxylic acid) were observed in much lower abundances, suggesting that NO<sub>x</sub> could contribute to the stability of the OH-acenaphthene adduct (Nishino et al., 2012). Conversely, products (i.e. acenaphthenone) from H-atom abstraction from the cyclopenta-fused ring pathway were observed in relatively higher abundance in both gas- and particulate



phases. Although, the (acenaphthene + OH) reaction proceeds through two different pathways under low- $\text{NO}_x$  conditions, it is difficult to distinguish which one dominates the global mechanism presented in Scheme 2. Previous studies have evaluated the competition between OH addition to the aromatic ring and H-atom abstraction (from aromatic rings) pathways: under atmospheric conditions the mechanism of reaction of OH radicals with aromatic hydrocarbons occurs mainly (i.e. > 90%) via addition to the aromatic ring (Calvert et al., 2002; Atkinson and Arey, 2007). Therefore, the results presented in this work suggest that the competition between OH-addition and H-atom abstraction from the cyclopenta-fused ring is more important than previously expected. Hence, the OH oxidation of acenaphthene could also be governed by H-atom abstraction from the cyclopenta-fused ring depending on the concentration of  $\text{NO}_x$ . More work is, however, needed to quantify the branching ratio between both pathways.

### 3.3 SOA formation.

Rapid SOA formation was observed in all experiments immediately after the formation of OH radicals. Using a semi-empirical model for SOA formation based on the gas-particle partitioning equilibrium of semi volatile products (Odum et al., 1996), the SOA yields ( $Y$ ), were determined from the experiments performed under low- /high- $\text{NO}_x$  conditions to be 0.61/0.46 and 0.68/0.55 for acenaphthylene and acenaphthene, respectively (Table 1). The volume concentration was corrected for particle wall loss by applying size-dependent first-order loss coefficients after SOA growth was finished. The indicated uncertainties ( $2\sigma$ ) in Table 1 correspond to scatter in particle volume measurements. The aerosol mass was calculated using volume concentrations measured by SMPS and assuming a particle density of  $1.4 \text{ g cm}^{-3}$  (Chan et al., 2009; Shakya and Griffin, 2010). The high concentrations used in this work probably enhanced partitioning of semi volatile species to the particle phase resulting in SOA yields that are larger than might be expected under more realistic atmospheric conditions. Nevertheless, the high yields determined in this work further illustrate the important potential of PAHs to form SOA from their oxidation by OH radicals. The first study reporting SOA formation yields from the photooxidation of acenaphthene and acenaphthylene under high- and low- $\text{NO}_x$  conditions was proposed by Shakya and Griffin (2010). The SOA yields proposed in the previous work (0.04-0.13 and 0.03-0.11 for acenaphthylene and acenaphthene photooxidation respectively) are much lower than those reported here. It is worth noting that, even though similar initial PAH concentrations were used, large discrepancies exist between the SOA yields reported by Chan et al. (2009) and

Shakya and Griffin (2010) for naphthalene photooxidation. Indeed, Shakya and Griffin (2010) proposed yields in the range of 0.08-0.16, while Chan et al. (2009) determined yields to be 0.19-0.74. As discussed by Chen et al. (2016), differences of SOA yields could be attributed to different chamber conditions such as light intensity, NO<sub>x</sub> levels, OH radicals, and organic mass loading. In the case of aromatic chemistry, it has been shown that photolysis processes play a major role in the loss of carbonyl products (Wang et al., 2006; Clifford et al., 2011). For instance, aromatic aldehydes can be photodissociated, leading to the formation of more oxidized compounds, which could further contribute to SOA formation (Wang et al., 2006). Furthermore, Warren et al. (2010) have reported the importance of light intensity in SOA formation from the photooxidation of monoaromatics. Therefore, in addition to the high concentration of PAHs, higher photolysis rates could also explain the subsequent SOA yields determined in this work.

Under high-NO<sub>x</sub> conditions, the photolysis of HONO generated relatively high concentrations of OH (i.e.  $8.4 \times 10^6$  molecule cm<sup>-3</sup>), leading to rapid acenaphthene and acenaphthylene consumption. Under low-NO<sub>x</sub> conditions, aerosol growth was also observed immediately after the lights were turned on. Nevertheless, the PAH consumption appeared to be slower than under high-NO<sub>x</sub> conditions, owing to the relatively low concentration of OH radicals produced by H<sub>2</sub>O<sub>2</sub> photolysis. Figure S1 presents the time-dependent growth curves (i.e. the mass of organic aerosol generated, noted as  $\Delta Mo$ , as a function of reacted PAH,  $\Delta HC$ ) for acenaphthene and acenaphthylene reactions with OH radicals under high- and low-NO<sub>x</sub> conditions. For all experiments, a constant increase of aerosol mass was observed and reached its maximum when acenaphthylene or acenaphthene was totally consumed. No clear difference was found between the high- and low-NO<sub>x</sub> conditions, indicating that compounds produced during the photooxidation of PAHs likely participate in SOA growth. Similar trends have been observed previously during the photooxidation of biogenic and anthropogenic precursors (Ng et al., 2006; Chan et al., 2009). The fact that aerosol growth stopped when the precursor was consumed indicates that the first oxidation reaction is the rate-determining step in SOA formation. In this case, the primary products could directly condense and participate in SOA formation, and therefore contribute to aerosol growth.

#### 4. Conclusion

In this work, both gas and particle phase products from the OH oxidation of acenaphthylene and acenaphthene were characterized using two on-line techniques (i.e. PTR-TOF-MS and



ATOFMS). The impact of  $\text{NO}_x$  on product distributions and SOA formation was explored for these compounds for the first time. Based on these results, extended mechanisms for the gas-phase oxidation of acenaphthylene and acenaphthene are proposed suggesting additional pathways and previously unidentified compounds under the conditions used in this work. The OH oxidation of acenaphthylene under high- and low- $\text{NO}_x$  conditions is mainly governed by OH addition. The significant production of products such as acenaphthenequinone or 1,8-naphthalic anhydride suggests preferential OH addition to the unsaturated cyclopenta-fused ring. On the contrary, acenaphthene oxidation begins with OH radical addition to the aromatic ring followed by the reaction of the resultant OH-adduct with  $\text{O}_2$  and further ring cleavages in the presence of  $\text{NO}_x$ . H-atom abstraction from the saturated cyclopenta-fused ring appears, however, not to be negligible as stipulated in previous work, especially in the absence of  $\text{NO}_x$ . Indeed, products from the H-atom abstraction pathway, such as acenaphthenone, exhibit a higher importance in the experiments performed in absence of  $\text{NO}_x$ . In addition, secondary chemistry was identified in all experiments and is now proposed in the extended mechanisms. The oxidation of acenaphthene and acenaphthylene formed SOA in large yields and suggest that the reaction of OH radicals with PAHs could contribute to anthropogenic SOA formation. It is shown that SOA growth is relatively linear and completes when the precursor hydrocarbon is consumed. Such observations illustrate that SOA formation is mainly due to the first generation products proceeding through gas-to-particle conversion processes. SOA formation yields are higher under low- $\text{NO}_x$  conditions than under high- $\text{NO}_x$  conditions as previously reported for the photooxidation of other aromatic compounds. Further experimental works on SOA formation from the photooxidation of acenaphthylene and acenaphthene is, however needed to better evaluate the impact of light intensity and  $\text{NO}_x$  mixing ratio on the different oxidation pathways.

## AUTHOR INFORMATION

Corresponding authors:

John C. Wenger

Email: j.wenger@ucc.ie

Phone: +353 21 490 3000

Eric Villenave

Email: e.villenave@epoc.u-bordeaux1.fr

Phone: +33 5 4000 6350

## ACKNOWLEDGEMENTS

Research at University College of Cork was supported by the EU-FP7 ‘European Simulation Chambers for Investigating Atmospheric Processes’ (EUROCHAMP-2, grant *number* 228335). The authors wish to thank the French Agency for Environment and Energy Management (ADEME) and the Aquitaine Region for their financial support.

## References

- Arey, J.; Zielinska, B.; Atkinson, R.; Aschmann, S.M. Nitroarene products from the gas-phase reactions of volatile polycyclic aromatic hydrocarbons with the OH radical and N<sub>2</sub>O<sub>5</sub>. *Int. J. Chem. Kinet.* **1989**, 21, 775–799.
- Atkinson, R.; Aschmann, S.M. Kinetics of the gas phase reactions of acenaphthene and acenaphthylene and structurally-related aromatic compounds with OH and NO<sub>3</sub> radicals, N<sub>2</sub>O<sub>5</sub> and O<sub>3</sub> at 296 ± 2 K. *Int. J. Chem. Kinet.* **1988**, 20, 513–539.
- Atkinson, R.; Arey, J. Atmospheric chemistry of gas-phase polycyclic aromatic hydrocarbons: Formation of atmospheric mutagens. *Environ. Health Persp.* **1994**, 102, 117–126.
- Atkinson, R.; Arey, J. Mechanisms of the gas-phase reactions of aromatic hydrocarbons and PAHs with OH and NO<sub>3</sub> radicals. *Polycycl. Aromat. Comp.* **2007**, 27, 15–40.
- Banceau, C.E.; Mihele, C.; Lane, D.A.; Bunce, N.J. Reactions of methylated naphthalenes with hydroxyl radicals under simulated atmospheric conditions. *Polycycl. Aromat. Comp.* **2001**, 18, 415–425.
- Brubaker Jr., W.W.; Hites, R.A. OH reaction kinetics of polycyclic aromatic hydrocarbons and polychlorinated dibenzo-p-dioxins and dibenzofurans. *J. Phys. Chem. A* **1998**, 102, 915–921.
- Calvert, J.G.; Atkinson, R.; Becker, K.H.; Kamens, R.M.; Seinfeld, J.H.; Wallington, T.J.; Yarwood, G. The mechanisms of atmospheric oxidation of aromatic hydrocarbons. *Oxford university press*, 2002, pp. 556.
- Cappelin, L.; Karl, T.; Probst, M.; Ismailova, O.; Winkler, P.M.; Soukoulis, C.; Aprea, E.; Märk, T.D.; Gasperi, F.; Biasioli, F. On quantitative determination of volatile organic compound concentration using proton transfer reaction time-of-flight mass spectrometry. *Environ. Sci. Technol.* **2012**, 46, 2283–2290.
- Chacon-Madrid, H.J.; Henry, K.M.; Donahue, N.M. Photo-oxidation of pinonaldehyde at low NO<sub>x</sub>: from chemistry to organic aerosol formation. *Atmos. Chem. Phys.* **2013**, 13, 3227–3236.
- Chan, A.W.H.; Kautzman, K.E.; Chhabra, P.S.; Surratt, J.D.; Chan, M.N.; Crounse, J.D.; Kürten, A.; Wennberg, P.O.; Flagan, R.C.; Seinfeld, J.H. Secondary organic aerosol formation from

photooxidation of naphthalene and alkylnaphthalenes: implications for oxidation of intermediate volatility organic compounds (IVOCs). *Atmos. Chem. Phys.* **2009**, 9, 3049–3060.

Chang, K.-F.; Fang, G.-C.; Chen, J.-C.; Wu, Y.-S. Atmospheric polycyclic aromatic hydrocarbons (PAHs) in Asia: a review from 1999 to 2004. *Environ. Pollut.* **2006**, 142, 388–396.

Chen, C.-L.; Kacarab, M.; Tang, P.; Cocker III, D.R. SOA formation from naphthalene, 1-methylnaphthalene, and 2-methylnaphthalene photooxidation. *Atmos. Environ.* **2016**, 131, 424–453.

Clifford, G.M.; Hadj-Aïssa, A.; Healy, R.M.; Mellouki, A.; Muñoz, A.; Wirtz, K.; Martín Reviejo, M.; Borrás, E.; Wenger, J.C. The atmospheric photolysis of o-tolualdehyde. *Environ. Sci. Technol.* **2011**, 40, 9649–9657.

Cox, R.A. The photolysis of nitrous acid in the presence of carbon monoxide and sulphur dioxide. *J. Photochem.* **1974**, 3, 291–304.

Dang, J.; Shi, X.; Zhang, Q.; Hu, J.; Wang, W. Mechanism and thermal rate constant for the gas-phase ozonolysis of acenaphthylene in the atmosphere. *Sci. Tot. Environ.* **2015**, 514, 344–350.

Dejean, S.; Raynaud, C.; Meybeck, M.; Della Massa, J.-P.; Simon, V. Polycyclic aromatic hydrocarbons (PAHs) in atmospheric urban area: monitoring on various types of sites. *Environ. Monit. Assess.* **2009**, 148, 27–37.

Ervens, B.; Turpin, B.J.; Weber, R.J. Secondary organic aerosol formation in cloud droplets and aqueous particles (aqSOA): A review of laboratory, field and model studies. *Atmos. Chem. Phys.* **2011**, 11, 11069–11102.

Estève, W.; Budzinski, H.; Villenave, E. Heterogeneous reactivity of OH radicals with phenanthrene. *Polycycl. Aromat. Comp.* **2003**, 23, 441–456.

Galloway, M.M.; Chhabra, P.S.; Chan, A.W.H.; Surratt, J.D.; Flagan, R.C.; Seinfeld, J.H.; Keutsch, F.N. Glyoxal uptake on ammonium sulphate seed aerosol: reaction products and reversibility of uptake under dark and irradiated conditions. *Atmos. Chem. Phys.* **2009**, 9, 3331–3345.

- 555 Gard, E.; Mayer, J.E.; Morrical, B.D.; Dienes, T.; Fergenson, D.P.; Prather, K.A. Real-time  
556 analysis of individual atmospheric aerosol particles: Design and performance of a portable  
557 ATOFMS. *Anal. Chem.* **1997**, 69, 4083–4091.
- 558
- 559 Gross, D.S.; Galli, M.E.; Silva, P.J.; Wood, S.H.; Liu, D.-Y.; Prather, K.A. Single particle  
560 characterization of automobile and diesel truck emissions in the Caldecott Tunnel. *Aerosol Sci.*  
561 *Technol.* **2000**, 32, 152–163.
- 562
- 563 Gross, D. S.; Barron, A. R.; Sukovich, E. M.; Warren, B. S.; Jarvis, J. C.; Suess, D. T.; Prather, K.  
564 A. Stability of single particle tracers for differentiating between heavy- and light-duty vehicle  
565 emissions. *Atmos. Environ.* **2005**, 39, 2889–2901.
- 566
- 567 Hallquist, M.; Wenger, J.C.; Baltensperger, U.; Rudich, Y.; Simpson, D.; Claeys, M.; Dommen, J.;  
568 Donahue, N.M.; George, C.; Goldstein, A.H.; Hamilton, J.F.; Herrmann, H.; Hoffmann, T.;  
569 Iinuma, Y.; Jang, M.; Jenkin, M.E.; Jimenez, J.L.; Kiendler-Scharr, A.; Maenhaut, W.;  
570 McFiggans, G.; Mentel, Th.F.; Monod, A.; Prévôt, A.S.H.; Seinfeld, J.H.; Surratt, J.D.;  
571 Szmigielski, R.; Wildt, J. The formation, properties and impact of secondary organic aerosol:  
572 current and emerging issues. *Atmos. Chem. Phys.* **2009**, 9, 5155–5236.
- 573
- 574 Hanedar, A.; Alp, K.; Kaynak, B.; Avsar, E. Toxicity evaluation and source apportionment of  
575 polycyclic aromatic hydrocarbons (PAHs) at three stations in Istanbul, Turkey. *Sci. Tot. Environ.*  
576 **2014**, 488, 437–446.
- 577
- 578 Healy, R.M.; Chen, Y.; Kourichev, I.; Kalberer, M.; O'Shea, D.; Wenger, J.C. Rapid formation of  
579 secondary organic aerosol from the photolysis of 1-nitronaphthalene: role of naphthoxy radical  
580 self-reaction. *Environ. Sci. Technol.* **2012**, 46, 11813–11820.
- 581
- 582 Ho, K.F.; Ho, S.S.H.; Lee, S.C.; Cheng, Y.; Chow, J.C.; Watson, J.G.; Louie, P.K.K.; Tian, L.W.  
583 Emissions of gas- and particle-phase polycyclic aromatic hydrocarbons (PAHs) in the Shing Mun  
584 Tunnel, Hong Kong. *Atmos. Environ.* **2009**, 43, 6343–6351.
- 585
- 586 Kautzman, K.E.; Surratt, J.D.; Chan, M.N.; Chan, A.W.H.; Hersey, S.P.; Chhabra, P.S.; Dalleska,  
587 N.F.; Wennberg, P.O.; Flagan, R.C.; Seinfeld, J.H. Chemical composition of gas- and aerosol-  
588 phase products from the photooxidation of naphthalene. *J. Phys. Chem. A* **2010**, 114, 913–934.
- 589
- 590 Keyte, I.J.; Harrison, R.M.; Lammel, G. Chemical reactivity and long-range transport potential of  
591 polycyclic aromatic hydrocarbons – a review. *Chem. Soc. Rev.* **2013**, 42, 9333–9391.

- Kleindienst, T.E.; Jaoui, M.; Lewandowski, M.; Offenberg, J.H.; Docherty, K.S. The formation of SOA and chemical tracer compounds from the photooxidation of naphthalene and its methyl analogs in the presence and absence of nitrogen oxide. *Atmos. Chem. Phys.* **2012**, 12, 8711–8726.
- Kourtchev, I.; Bejan, I.; Sodeau, J.R.; Wenger, J.C. Gas-phase reaction of (E)- $\beta$ -farnesene with ozone: Rate coefficient and carbonyl products. *Atmos. Environ.* **2009**, 43, 3182–3190.
- Kroll, J.H.; Seinfeld, J.H. Chemistry of secondary organic aerosol: formation and evolution of low-volatility organics in the atmosphere. *Atmos. Environ.* **2008**, 42, 3593–3624.
- Lee, J.Y.; Lane, D.A. Unique products from the reaction of naphthalene with the hydroxyl radical. *Atmos. Environ.* **2009**, 43, 4886–4893.
- Lin, P.-H.; Pan, W.-C.; Kang, Y.-W.; Chen, Y.-L.; Lin, C.-H.; Lee, M.-C.; Chou, Y.-H.; Nakamura, J. Effects of naphthalene quinonoids on the induction of oxidative DNA damage and cytotoxicity in calf thymus DNA and in human cultured cells. *Chem. Res. Toxicol.* **2005**, 18, 1262–1270.
- Marais, E.A.; Jacob, D.J.; Jimenez, J.L.; Campuzano-Jost, P.; Day, D.A.; Hu, W.; Krechmer, J.; Zhu, L.; Kim, P.S.; Miller, C.C.; Fisher, J.A.; Travis, K.; Yu, K.; Hanisco, T.F.; Wolfe, G.M.; Arkinson, H.L.; Pye, H.O.T.; Froyd, K.D.; Liao, J.; McNeill, V.F. Aqueous-phase mechanism for secondary organic aerosol formation from isoprene: application to the southeast United States and co-benefit of SO<sub>2</sub> emission controls. *Atmos. Chem. Phys.* **2016**, 16, 1603–1618.
- March, J. Advanced Organic Chemistry, 3rd ed.; *John Wiley & Sons*: New York, 1985; pp 66–68.
- Ng, N.L.; Kroll, J.H.; Keywood, M.D.; Bahreini, R.; Varutbangkul, V.; Flagan, R.C.; Seinfeld, J.H.; Lee, A.; Goldstein, A.H. Contribution of first- versus second-generation products to secondary organic aerosols formed in the oxidation of biogenic hydrocarbons. *Environ. Sci. Technol.* **2006**, 40, 2283–2297.
- Nishino, N.; Arey, J.; Atkinson, R. 2-Formylcinnamaldehyde formation yield from the OH radical-initiated reaction of naphthalene: effect of NO<sub>2</sub> concentration. *Environ. Sci. Technol.* **2012**, 46, 8198–8204.
- Odum, J.R.; Hoffmann, T.; Bowman, F.; Collins, D.; Flagan, R.C.; Seinfeld, J. H. Gas/particle partitioning and secondary organic aerosol yields. *Environ. Sci. Technol.* **1996**, 30, 2580–2585.

- Pope III, C.A.; Dockery, D.W. Health effects of fine particulate air pollution: lines that connect. *J. Air Waste Manage. Assoc.* **2006**, 56, 709–742.
- Pye, H.O.T.; Pouliot, G.A. Modeling the role of alkanes, polycyclic aromatic hydrocarbons, and their oligomers in secondary organic aerosol formation. *Environ. Sci. Technol.* **2012**, 46, 6041–6047.
- Pye, H.O.T.; Pinder, R.W.; Piletic, I.R.; Xie, Y.; Capps, S.L.; Lin, Y.-H.; Surratt, J.D.; Zhang, Z.; Gold, A.; Luecken, D.J.; Hutzell, W.T.; Jaoui, M.; Offenberg, J.H.; Kleindienst, T.E.; Lewandowski, M.; Edney, E.O. Epoxide pathways improve model predictions of isoprene markers and reveal key role of acidity in aerosol formation. *Environ. Sci. Technol.* **2013**, 47, 11056–11064.
- Reisen, F.; Arey, J. Reactions of hydroxyl radicals and ozone with acenaphthene and acenaphthylene. *Environ. Sci. Technol.* **2002**, 36, 4302–4311.
- Riva, M.; Healy, R.M.; Flaud, P.-M.; Perraudin, E.; Wenger, J.C.; Villenave, E. Kinetics of the gas-phase reactions of chlorine atoms with naphthalene, acenaphthene and acenaphthylene. *J. Phys. Chem. A* **2014**, 118, 3535–3540.
- Riva, M.; Healy, R.M.; Flaud, P.-M.; Perraudin, E.; Wenger, J.C.; Villenave, E. Gas- and particle-phase products from the chlorine-initiated oxidation of polycyclic aromatic hydrocarbons. *J. Phys. Chem. A* **2015a**, 119, 11170–11181.
- Riva, M.; Robinson, E.S.; Perraudin, E.; Donahue, N.M.; Villenave, E. Photochemical aging of secondary organic aerosols generated from the photooxidation of polycyclic aromatic hydrocarbons in the gas-phase. *Environ. Sci. Technol.* **2015b**, 49, 5407–5416.
- Riva, M.; Tomaz, S.; Cui, T.; Lin, Y.-H.; Perraudin, E.; Gold, A.; Stone, E. A.; Villenave, E.; Surratt, J.D. Evidence for an unrecognized secondary anthropogenic source of organosulfates and sulfonates: gas-phase oxidation of polycyclic aromatic hydrocarbons in the presence of sulfate aerosol. *Environ. Sci. Technol.* **2015c**, 49, 6654–6664.
- Riva, M.; Healy, R.M.; Tomaz, S.; Flaud, P.-M.; Perraudin, E.; Wenger, J.C.; Villenave, E. Gas- and particulate phase products from the ozonolysis of acenaphthylene. *Atmos. Environ.* **2016**, 142, 104–113.



- Robinson, A.L.; Donahue, N.M.; Shrivastava, M.K.; Weitkamp, E.; Sage, A.M.; Grieshop, A. P.; Lane, T.E.; Pierce, J.R.; Pandis, S.N. Rethinking organic aerosols: semivolatile emissions and photochemical aging. *Science* **2007**, 315, 1259–1262.
- Sasaki, J.; Aschmann, S.M.; Kwok, E.S.C.; Atkinson, R.; Arey, J. Products of the gas-phase OH and NO<sub>3</sub> radical-initiated reactions of naphthalene. *Environ. Sci. Technol.* **1998**, 31, 3173–3179.
- Sauret-Szczepanski, N.; Lane, D.A. Smog chamber study of acenaphthene: gas-particle partition measurements of the products formed by reaction with the OH radical. *Polycycl. Aromat. Comp.* **2004**, 24, 161–172.
- Shakya, K.M.; Griffin, R.J. Secondary organic aerosol from photooxidation of polycyclic aromatic hydrocarbons. *Environ. Sci. Technol.* **2010**, 44, 8134–8139.
- Silva, P.J.; Prather, K.A. Interpretation of mass spectra from organic compounds in aerosol time-of-flight mass spectrometry. *Anal. Chem.* **2000**, 72, 3553–3562.
- Surratt, J.D.; Gomez-Gonzalez, Y.; Chan, A.W.H.; Vermeylen, R.; Shahgholi, M.; Kleindienst, T.E.; Edney, E.O.; Offenberg, J.H.; Lewandowski, M.; Jaoui, M.; Maenhaut, W.; Claeys, M.; Flagan, R.C.; Seinfeld, J.H. Organosulfate formation in biogenic secondary organic aerosol. *J. Phys. Chem. A* **2008**, 112, 8345–8378.
- Thüner, L.P.; Bardini, P.; Rea, G.J.; Wenger, J.C. Kinetics of the gas-phase reactions of OH and NO<sub>3</sub> radicals with dimethylphenols. *J. Phys. Chem. A* **2004**, 108, 11019–11025.
- Tkacik, D.S.; Presto, A.A.; Donahue, N.M.; Robinson, A.L. Secondary organic aerosol formation from intermediate-volatility organic compounds: cyclic, linear, and branched alkanes. *Environ. Sci. Technol.* **2012**, 46, 8773–8781.
- Volkamer, R.; Jimenez, J.L.; San Martini, F.; Dzepina, K.; Zhang, Q.; Salcedo, D.; Molina, L.T.; Worsnop, D.R.; Molina, M.J. Secondary organic aerosol formation from anthropogenic air pollution: Rapid and higher than expected. *Geophys. Res. Lett.* **2006**, 33, L17811.
- Wang, L.; Arey, J.; Atkinson, R. Kinetics and products of photolysis and reaction with OH radicals of a series of aromatic carbonyl compounds. *Environ. Sci. Technol.* **2006**, 40, 5465–5471.



- Warren, B.; Song, C.; Cocker, D.R. Light intensity and light source influence on secondary organic aerosol formation for the *m*-xylene/NO<sub>x</sub> photooxidation system. *Environ. Sci. Technol.* **2008**, 42, 5461–5466.
- Zander, M. Notiz über dimere biacenaphthylenyl-(1.1') („Di-perinaphthylenbutadien“). *Chem. Ber.* **1969**, 102, 3599–3602.
- Zelenyuk, A.; Imre, D. Single particle laser ablation time-of-flight mass spectrometer: An introduction to SPLAT. *Aerosol Sci. Tech.* **2005**, 39, 554–568.
- Zhou, S.; Wenger, J.C. Kinetics and products of the gas-phase reactions of acenaphthene with hydroxyl radicals, nitrate radicals and ozone. *Atmos. Environ.* **2013a**, 72, 97–104.
- Zhou, S.; Wenger, J.C. Kinetics and products of the gas-phase reactions of acenaphthylene with hydroxyl radicals, nitrate radicals and ozone. *Atmos. Environ.* **2013b**, 75, 103–112.
- Zimmermann, R.; Ferge, T.; Galli, M.; Karlsson, R. Application of single-particle laser desorption/ionization time-of-flight mass spectrometry for detection of polycyclic aromatic hydrocarbons from soot particles originating from an industrial combustion process. *Rapid Commun. Mass Spectrom.* **2003**, 17, 851–859.

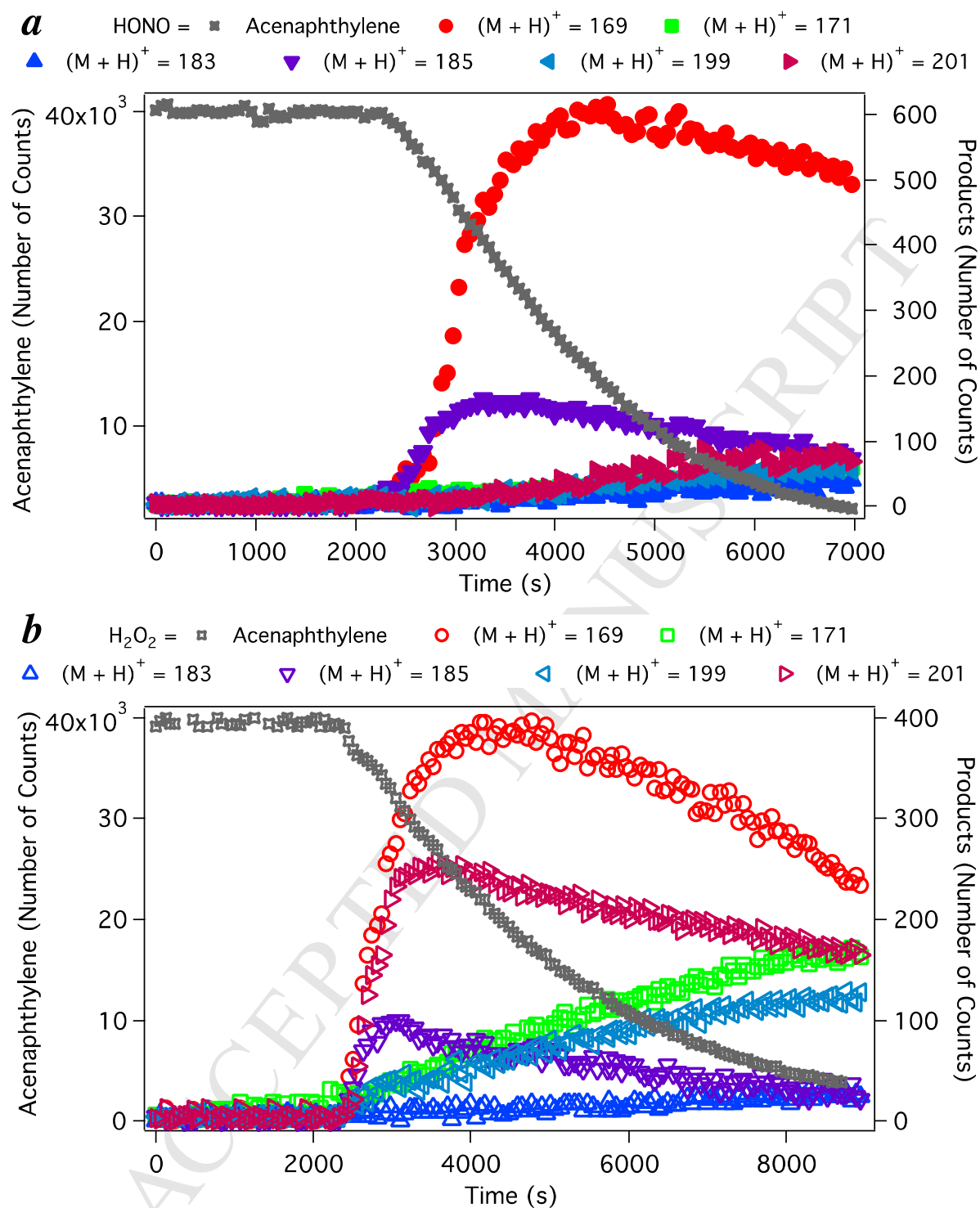


**Figure 1.** Temporal profiles of major ions identified by PTR-TOF-MS from the gas-phase oxidation of acenaphthylene initiated by OH radicals (full and open markers represent experiments performed under high- (a) and low-NO<sub>x</sub> (b) conditions, respectively).

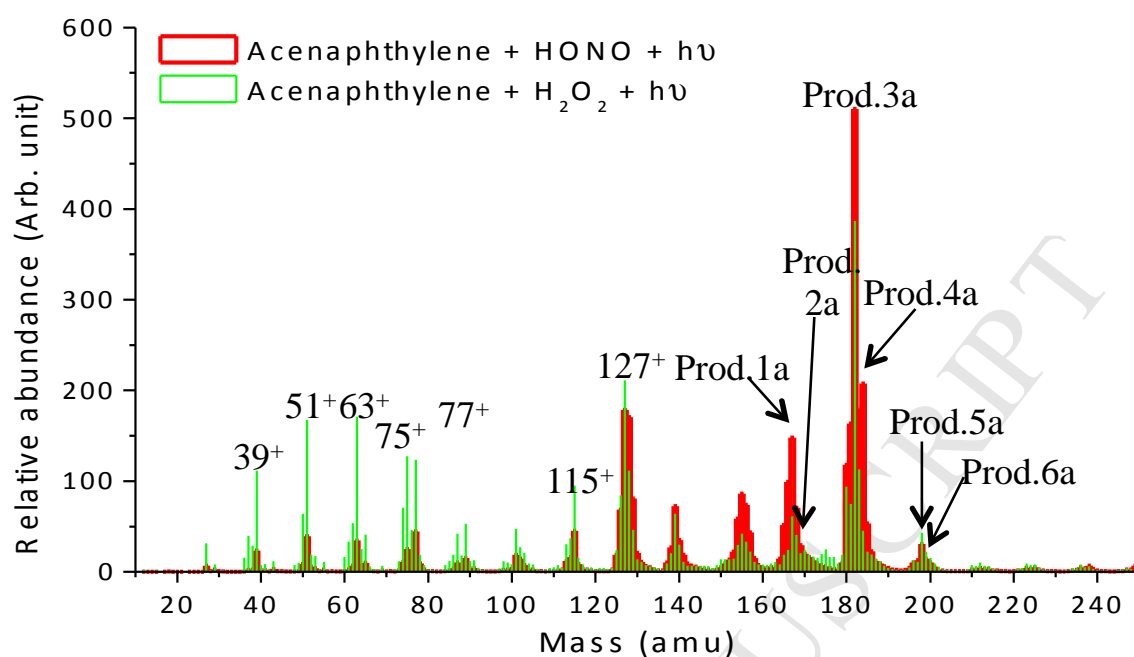


**Figure 2.** ATOFMS average mass spectra (positive ion mode) using a laser pulse of 0.2 mJ for SOA formed from the photooxidation of acenaphthylene under high- (red) and low-NO<sub>x</sub> (green) conditions.

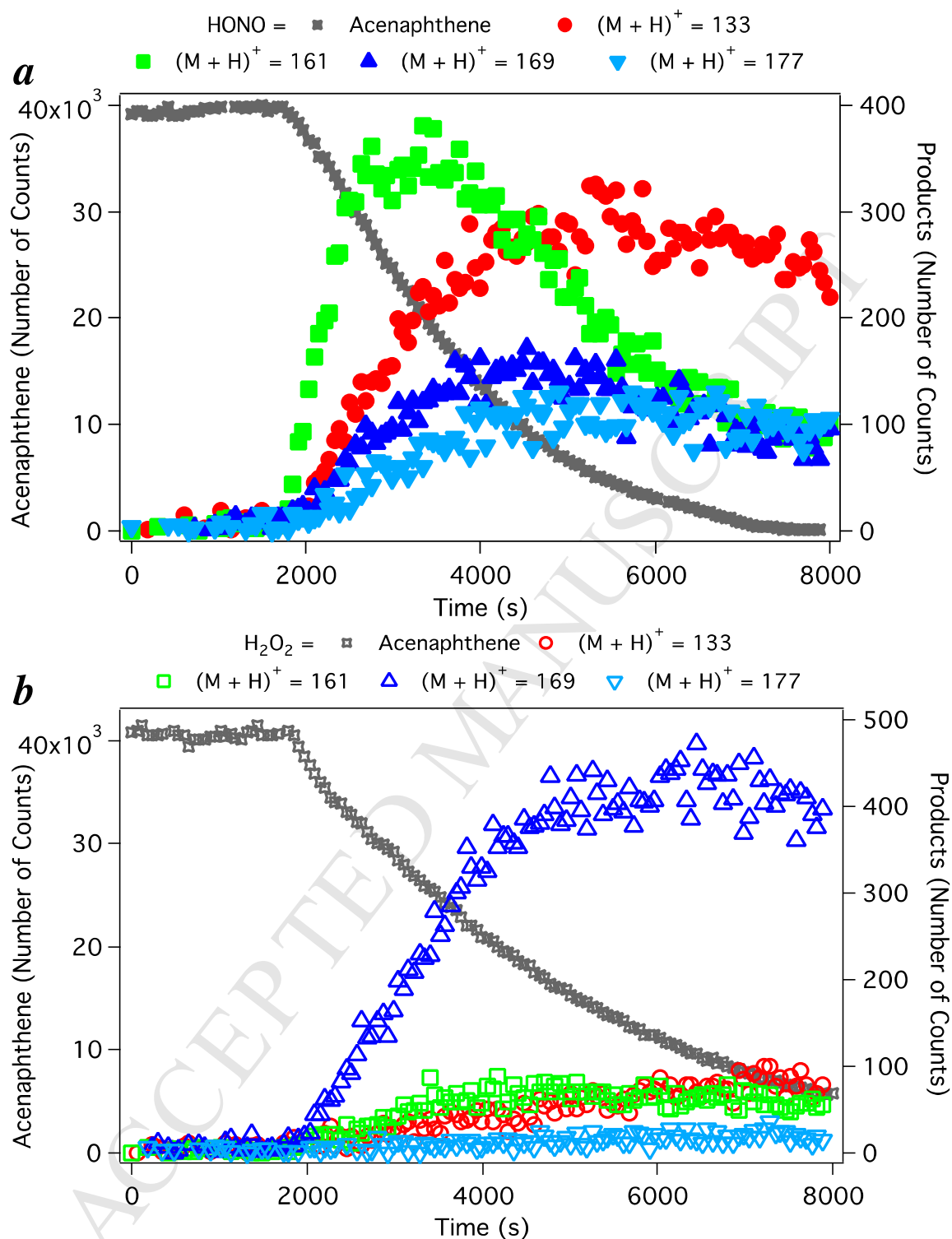


**Figure 3.** Main gas-phase compounds identified during the photooxidation of acenaphthene using PTR-TOF-MS (full and open markers represent experiments performed under high- (a) and low-NO<sub>x</sub> (b) conditions, respectively).

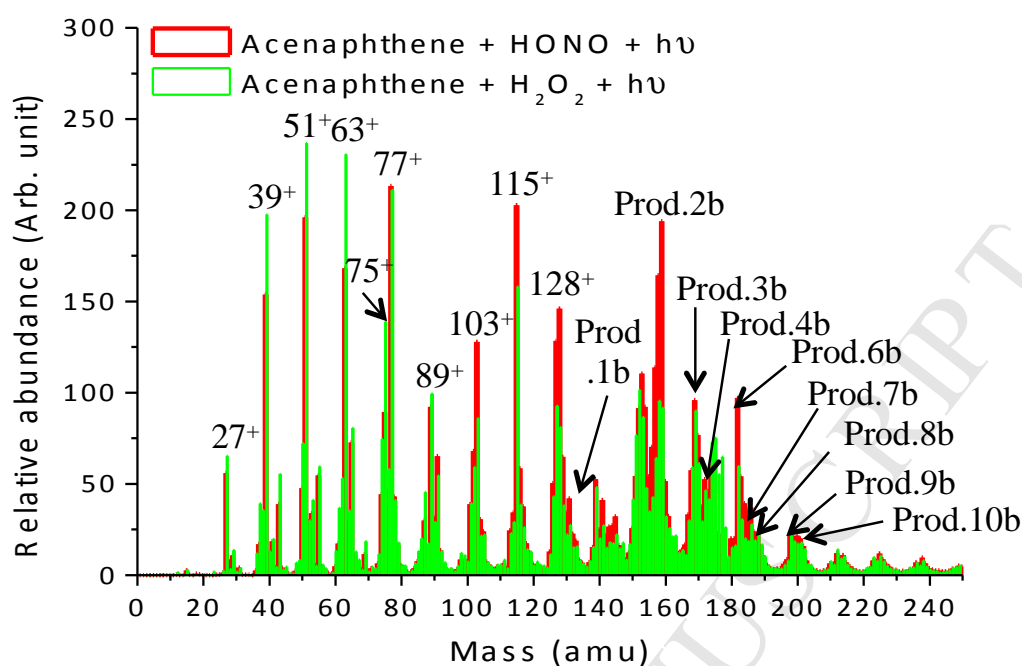
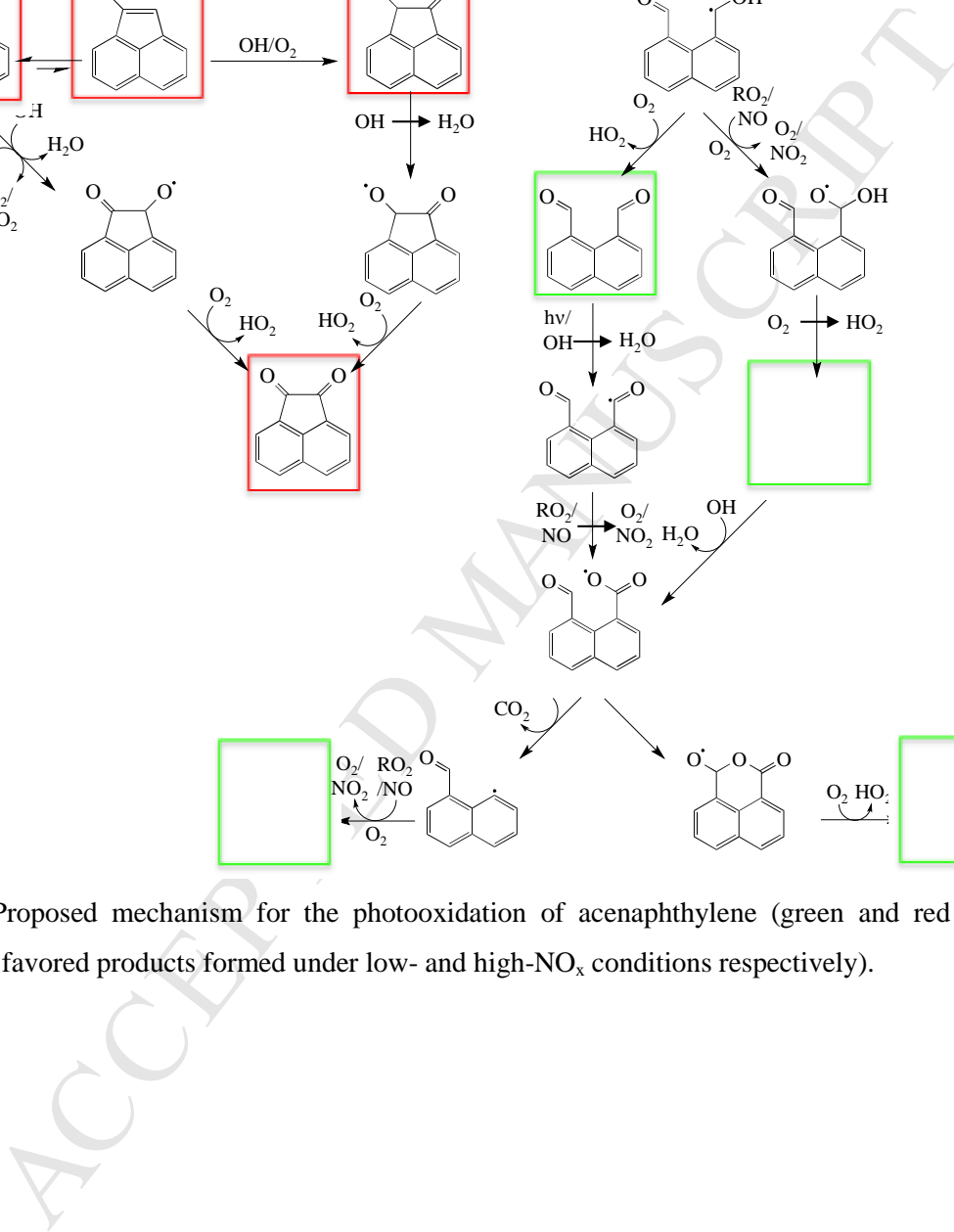
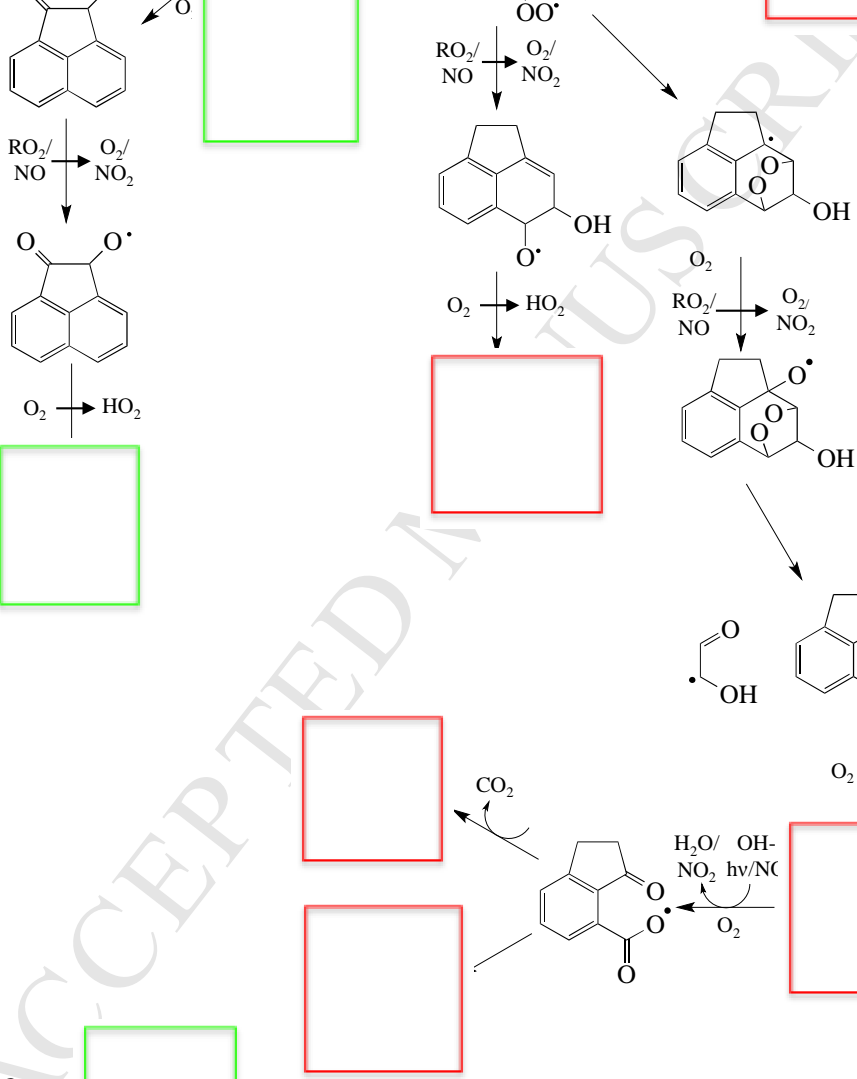


**Figure 4.** ATOFMS average mass spectra (positive ion mode) using a laser pulse of 0.2 mJ for SOA formed from the photooxidation of acenaphthene under high- (red) and low-NO<sub>x</sub> (green) conditions.



represent the favored products formed under low- and high-NO<sub>x</sub> conditions respectively).



743  
744  
745

**HIGHLIGHTS**

Identification of competitive pathways for the OH-initiated oxidation of Acenaphthene

Formation of ring-opening products favored from the OH oxidation of Acenaphthylene

Impact of NO<sub>x</sub> on product distributions and SOA formation have been observed

Proposition of identified secondary chemistry in the extended mechanisms

SOA yields in the range 46-68% have been measured